Multiple Bonding Interactions in Dimeric Hetero-closo-dodecaborates of Group-14 Elements – A Theoretical Study

Brindha Veerappan

Department of Chemistry (SF), PSG College of Arts and Science

Krishnamoorthy Bellie Sundaram

bskimo@yahoo.co.in

Department of Chemistry (SF), PSG College of Arts and Science

Research Article

Additional Declarations: No competing interests reported.

Multiple Bonding Interactions in Dimeric Hetero-*closo*-dodecaborates of Group-14 Elements – A Theoretical Study

Brindha Veerappan[1] and Krishnamoorthy Bellie Sundaram[1]*

[1] Department of Chemistry (SF), PSG College of Arts and Science, Coimbatore, Tamil Nadu, India. 641014.

Correspondence: bskimo@yahoo.co.in; 0091-9585447505;

Abstract

Context The geometric and electronic structural futures of group-14 hetero-*closo*-dodecaborates such as monomers $[EB_{11}H_{11}]^{1-}$, $[EB_{11}H_{11}]^{2-}$ and dimers $[(EB_{11}H_{11})_2]^{2-}$ [E = C, Si, Ge, Sn and Pb] is analyzed using density functional theory (DFT) method. The structural feature such as metrical parameters and binding interactions are theoretically studied. The dispersion correction method has been used to get more insight. The dispersion correction method improves the metrical parameter of group-14 elements towards experimental parameters. The electronic structure of the clusters has been studied using frontier molecular orbital analysis (FMO). It shows the group-14 elements electronic contribution and possible electron delocalization between the cages to stabilize the dimeric clusters. The thermochemistry from numerical frequency analysis suggests the plausible and synthetic viability of the dimeric clusters. The spectroscopic studies (^{1}H, ^{11}B, ^{13}C and ^{119}Sn) elucidate the structures of the cluster with chemical shifts (δ) of lower belt, upper belt and apical boron vertices. The global reactive descriptors and local descriptors are calculated to analyze the philicity of the clusters. According to the descriptor analysis, an identification of reactive sites with respect to an electrophilic and nucleophilic centers of the reactant has been reported.

Methods The density functional BP86 with Grimm's dispersion correction DFT-D3 method has been used to study the bonding interactions of group-14 hetero-*closo*-dodecaborate dimers. And, the Def2-TZVP basis set applied to this cluster system to investigate electronic structural features using ORCA software (v 5.0.4).

Keywords Heteroborate dimers . DFT . DFT-D3 . group-14. Stannaborane. Icosahedral Borane.

1 Introduction

Multiple bonding interactions between group 14 elements have unique electronic structure and bonding, [1-5] it specifically attracts most of the theoretical researchers especially through density functional theory (DFT) method. [6-8] The bonding interactions of RE ~ ER [(~ → -, =, ≡), (E = C, Si, Ge, Sn, Pb)] molecules are studied by Shigeru Nagase et al.[9] The heavier group multiple bonds are calculated by using Grimms dispersion correction D3 method.[10]

Icosahedral heteroborates are the kind of lewis acid-base in which the electrophilicity and nucleophilicity of the clusters are depends upon the heteroatoms.[11,12] The local descriptor and global reactive descriptors are key factors to determine the chemical nature of the system.[13-16] The amphiphilic nature is that the system has both nucleophilic and electrophilic nature.[16-18] This factor is mainly determined by Fukui functions, the global reactive descriptors such as chemical potential (μ), hardness (Π), softness (S) and electrophilicity (ω). These descriptors can be successfully calculated by using DFT method.[17,19] The chemical softness and hardness plays a major role in the behavior of the system, this concept firstly introduced by Robert S. Mulliken at 1952.[20] Then Hard and Soft Acid Base HSAB principle evolved by Pearson postulates. The absolute hardness was introduced by Pearson and Parr. Then Pearson published maximum hardness principle MHP, theses two MHP and HSAB used for the hardness and chemical potential. The Koopmann's theorem mainly used to derive the global reactive descriptors.[21] According to Koopmann's theorem, we can calculate the adiabatic ionization potential (AIP) and vertical ionization potential (VIP). The first ionization energy is derived from the highly occupied molecular orbitals (HOMO), the negative value of the highly occupied molecular orbital's energy plus the electrostatic potential energy of the electron removed from the

system. Similarly, we can calculate the ionization potential (IP) average of the highly occupied molecular orbitals (HOMO) of the neutral system (N) and the lowest unoccupied molecular orbitals (LUMO) of the cationic system (N-1). [22]
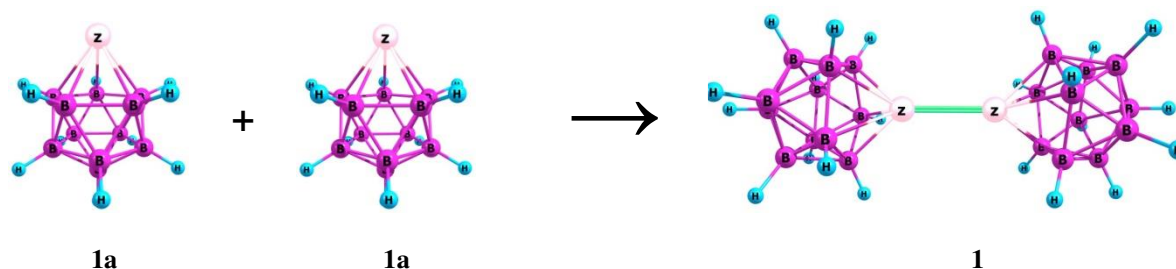
Scheme 1. The schematic diagram representing the molecules studied [z = C (1a), Si (2a), Ge (3a), Sn (4a), Pb (5a)]

Dimeric cluster of group-14 icosahedral geometry reported in 2015 by Wesemann et al, this is the first synthesized hetero-*closo*-dodecaborate dimer $[Bu_3MeN]_2[(GeB_{11}H_{11})_2]$, a clourless crystalline solid by the oxidation of germa-*closo*-dodecaborate using iodine and ferrocenium hexafluorophosphate. The dimer is dianionic in nature with the structural formula $[(GeB_{11}H_{11})_2]^{2-}$. [23] Here we have studied the monomers **1a-5a** and their corresponding dimers **1-5** using the DFT method to analyze their molecular structural features, stability and bonding interactions (**Scheme 1**). The *closo*-heteroborates are optimized by using BP86/Def2-TZVP level and the interactions are studied by D3BJ method.

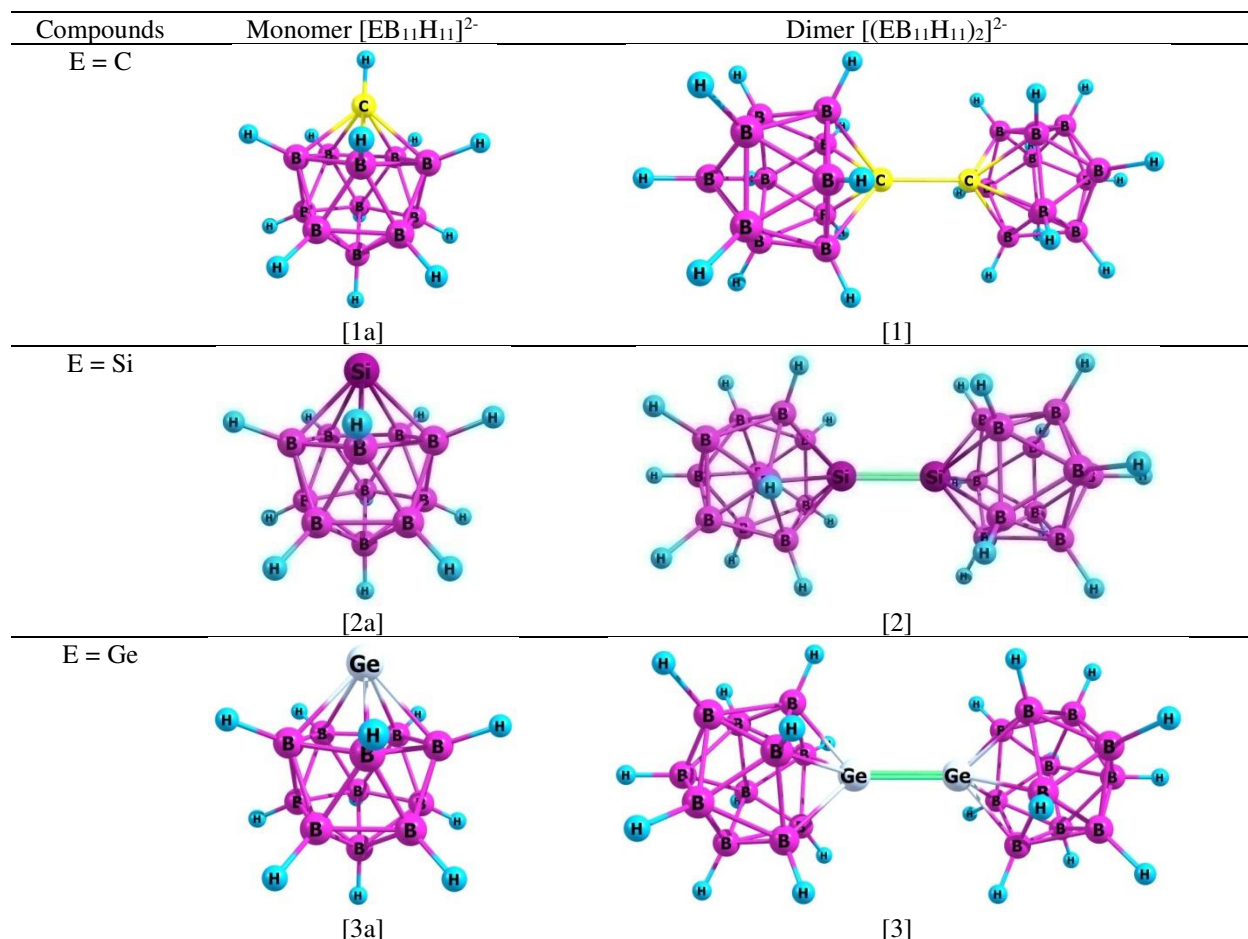## 2 Theoretical methodology and computational details

Computational chemistry techniques are increasingly being used as valuable tools to help with both the modeling of novel compounds and the complete structural characterization of existing compounds.[24-26] The following approaches were used to study each of the clusters: the normal optimization studied by usual DFT method at BP86/Def2-TZVP level, Molecular bonding analysis, frequency computation, NMR property calculation and reactivity descriptor analysis. All of the density functional theory computations in this work were done using ORCA software created by F. Neese and colleagues.[27] From the Vosko-Wilk-Nusair parameterization, [28] the Becke88 gradient correction for exchange and Perdew86 correlation inside the local density approximation (LDA) were applied.[29-31] The DFT functional BP86 highly favors the theoretical values with experimental values in metallaboranes. [12,32-34] For each clusters, the Def2-TZVP (triple zeta valance with polarization function) basis set was employed. TightSCF convergence requirements were used to every calculation.[35] The bonding interactions of group-14 elements are analyzed by using DFT-D3 method. The Grimm's dispersion correction D3 [36] with BJ (Beck-Johnson) damping [37-39] has been used to approach the closer value of experimental values for the heavy atom system. [9, 10] Using the ORCA software's EPRNMR module, the DFT-optimized geometries were utilized to compute NMR parameters such as chemical shifts and shielding constants.[40] The tetramethylsilane(TMS) has been used as reference compound, for computing ^1H and ^{13}C nmr chemical shift values.[41] The calculated ^{11}B NMR chemical shift values were translated to the standard $BF_3.OEt_2$ scale using the experimental value of +16.6 ppm for B_2H_6, with B_2H_6 serving as the major reference point.[41,42] The idea of generalized philicity was first presented by Chattaraj et al. It includes information on the electronphilic/nucleophilic power of a specific atomic location in a molecule, as well as nearly all of the previously known various global and local reactivity and selectivity characteristics. [43,44]
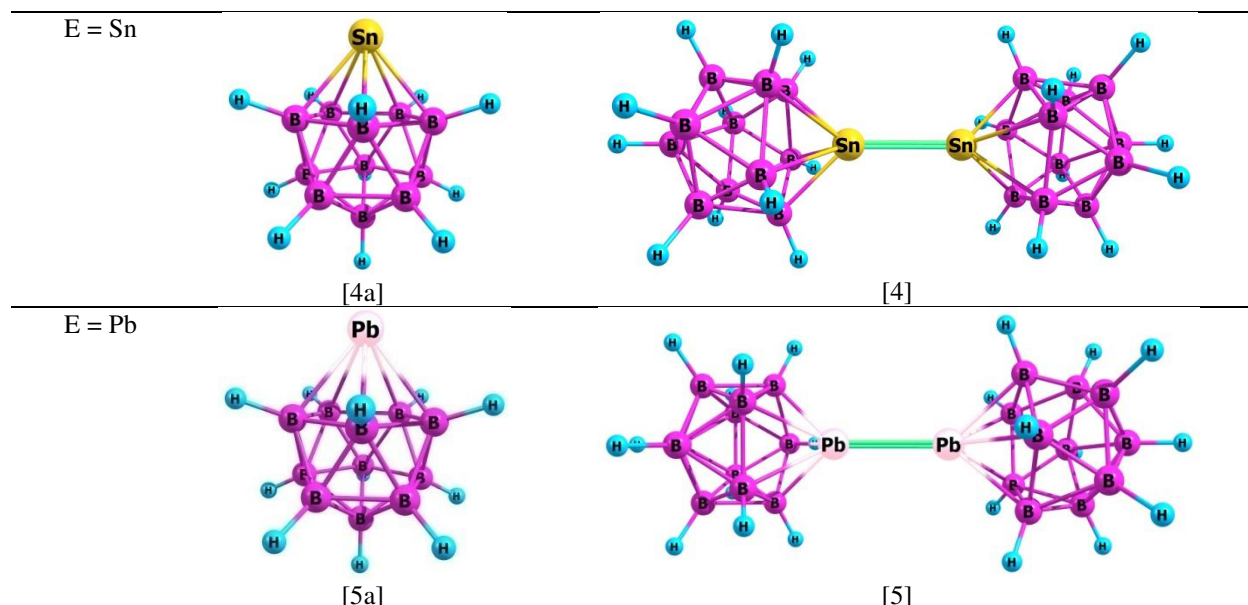
3 Results and Discussion

3.1 Geometrical Structure

The geometrical structures of the group-14 clusters are studied by using BP86/Def2-TZVP level. The optimized geometries are given in **Figure 1.** We have optimized monomers and its respective dimers of the group-14 *closo*-dodecaborates. The DFT(BP86/Def2-TZVP) computed metrical parameters and dispersion corrected values of heteroborane monomers (**1a-5a**) are provided in **Table S1** and **Table S2** respectively. Similarly the DFT(BP86/Def2-TZVP) computed metrical parameters and dispersion corrected values of heteroborane dimers (**1-5**) are provided in **Table S3** and **Table S4** respectively. The bonding interactions of E(Group-14) and B atoms are around 1.71Å for $[CB_{11}H_{11}]^{2-}$, 2.13 Å for $[SiB_{11}H_{11}]^{2-}$, 2.22 Å for $[GeB_{11}H_{11}]^{2-}$, 2.40 Å for $[SnB_{11}H_{11}]^{2-}$ and 2.49 Å for $[PbB_{11}H_{11}]^{2-}$. The order of increasing bond length is 1a < 2a < 3a < 4a < 5a, the increasing order depends upon the increasing the radii of group-14 elements and interatomic repulsions between B and group-14. The dispersion correction method (D3BJ) improves the bonding interactions which is highly agreement with experimental values. The increasing order of bonding interactions of E and B atoms of D3BJ method is 1.71 [1a] < 2.13 [2a] < 2.21 [3a] < 2.40 [4a] < 2.48 [5a] Å.

Figure 1. DFT optimized geometries of group-14 hetero-*closo*-dodecaborate monomers and dimmers at BP86/Def2-TZVP level.

Compounds	Monomer $[EB_{11}H_{11}]^{2-}$	Dimer $[(EB_{11}H_{11})_2]^{2-}$
E = C	[1a]	[1]
E = Si	[2a]	[2]
E = Ge	[3a]	[3]

E = Sn		
	[4a]	[4]
E = Pb		
	[5a]	[5]

The dimeric clusters have E=E bonding interactions with 1.55, 2.33, 2.40, 2.74 and 2.87Å for the clusters **1-5** respectively. The dispersion corrected E=E interactions are 1.54, 2.30, 2.37, 2.70 and 2.82 Å. The experimental values of the E=E bond of Ge dimer is 2.329(1) Å, which is very close to the DFT computed value of 2.370 Å the remaining compounds are not synthesized yet.[23] So, we have compared the related compounds experimental values for the clusters 1, 2, 4 and 5. The C-C interactions are similar to the alkanes bond distance around 1.54 Å, [45] confirming the single bond nature. DFT computed Si=Si bond length of 2.33 Å is similar to 2.16 Å, [46-47]. The DFT computed Sn=Sn double bond distance 2.6986 Å is very close to the stannylene double bond 2.668 Å. [48] The DFT computed Pb=Pb bond length of 2.820 Å is 0.124 Å longer than the experimentally known Pb=Pb bond in plumbene (2.696 Å). [9] All the dispersion corrected binding interactions are in good agreement with experimental values and related experimental values (**Table S5**). The experimentally available structure for stannaborate is $[(SnB_{11}H_{11})(SnB_{11}H_{10})]^{3-}$,[23] and the two stannaborate clusters are inter-connected by 'Sn-B' bonding with 2.2878 Å interatomic distance. The dispersion corrected (D3BJ) 'Sn-B' bond distance is 2.2457 Å. The spectroscopic values are in good agreement with the experimental values.

3.2 Chemical Descriptors

The chemical descriptors are the indicators of the of the molecules nature such as reactivity and reactive centre. The frontier molecular orbitals (FMO) of the clusters studied are provided in the **Figure SF1- Figure SF5**. Those are divided into two categories, local descriptors like highly occupied molecular orbitals (HOMO), lowest unoccupied molecular orbitals (LUMO), energy gap (ΔE) and global reactive descriptors like chemical potential (μ), hardness (Ӆ), softness (S), electrophilicity (ω), dipole moment, ionization potential (I_P), electron affinity (E_A). These parameters are calculated by using E_{HOMO} and E_{LUMO}. All these descriptors are the major key factor for the identifying the natures of the clusters. These descriptors are derived by using Koopmann's theorem.

3.2.1 Local Descriptors

We have computed (**Table 1**) the descriptors for monomers (**1a, 2a, 3a, 4a and 5a**) and dimers (**1, 2, 3, 4 and 5**). The energy gap determines the reactivity and kinetic stability of the geometry, energy of the group-14 monomers are around 3.8368 to 6.4526 eV. The energy gap range of group-14 dimer is 1.5361 to 6.3217 eV with highest E_{LUMO-}

HOMO energy gap values of 6.3 eV for carborane dimer cluster **1**. The increasing order of energy gap for monomer is **5a < 4a < 3a < 2a < 1a** and the dimer is **5 < 4 < 3 < 2 < 1.** The increasing order shows that the size of the group-14 element increases the energy gap of the clusters decreases.

Fukui function has been used to calculate the local descriptors and reactivity sites. Hirsh field analysis lead to the local philicity of the system from which we can determine either it is nucleophilic, electrophilic, neutral or amphiphilic in nature. The following equations 1, 2 and 3 have been used to calculate nucleophilic, electrophilic and radical attack.[17]

$$f_k^+ = q_k(N + 1) - q_k(N) \qquad\qquad \rightarrow 1$$

$$f_k^- = q_k(N) - q_k(N - 1) \qquad\qquad \rightarrow 2$$

$$f_k^o = [q_k(N + 1) - q_k(N - 1)]/2 \qquad\qquad \rightarrow 3$$

The dimerization of germa-*closo*-dodecaborate gives the dimeric 'Ge=Ge' bonded $[(GeB_{11}H_{11})]^{2-}$ cluster. But, in the case of stanna-*closo*-dodecaborate produces the 'Sn-B' bonded $[(SnB_{11}H_{11})(SnB_{11}H_{10})]^{3-}$ cluster. The quantum chemical computation favours the remaining group-14 dimeric product. The stanna-*closo*-dodecaborate computation posses the favourable results for both the Sn-B' and 'Sn=Sn' bonded cluster system. But, the energy gap for the 'Sn-B' system is 4.13 eV with 8.55 Debye dipole moment and 2.80 eV for the 'Sn=Sn' bonded system. The energy difference for these two systems is around 2 eV. So, we have done Fucki function analysis to determine the yield range of product.

The calculation of electrophilic Fukui function (f_k^+), nuclophilic Fukui function (f_k^-) and neutral Fukui function (f_k^o) through N-1, N+1 and N systems. The calculation shows that the f^-K, f^oK favours the B2 vertex with -0.0190, -0.0197 and f^+K favours B4 vertex with -0.0197. So, B2 and B4 vertex is electrophilic and nucleophic respectively, in nature. So, this analysis highly favours the 'Sn-B' bonded $[(SnB_{11}H_{11})(SnB_{11}H_{10})]^{3-}$ cluster formation. But, in the tin vertex, the calculations gives f^+K, f^-K and f^oK -0.5402, -0.2689 and -0.4046. Hence, tin vertex is highly nucleophilic in nature and less electrophilic nature. So, the 'Sn=Sn' bonded dimeric cluster is less favoured.

3.2.2 Global Reactive Descriptors

The global reactive descriptors are calculated by using below equations 4 to 8, the equation solved by using frontier molecular orbital HOMO and LUMO. [24] The DFT computed chemical descriptors are given in **Table 1**.

$$\text{Electronegativity} = -\frac{1}{2}(E_{LUMO}+E_{HOMO}) \qquad\qquad \rightarrow 4$$

$$\text{Global Chemical Potential } (\mu) = \frac{1}{2}(E_{LUMO}+E_{HOMO}) \qquad\qquad \rightarrow 5$$

$$\text{Global Hardness } (\eta) = \frac{1}{2}(E_{LUMO}- E_{HOMO}) \qquad\qquad \rightarrow 6$$

$$\text{Global Softness(S)} = 1/\eta \qquad\qquad \rightarrow 7$$

$$\text{Global Electrophilicity } (\omega) = \frac{\mu 2}{2\eta} \qquad\qquad \rightarrow 8$$

Chemical potential (μ) of the cluster carborane (1a) and plumbaborane (5) has very lower values -0.0934 and 0.0251, the lowest value obtained due to higher nucleophilicity of the cluster. The monomers have the higher (μ) value than the dimmers except carborane system. It determines that the dimmers are highly nucleophilic in nature than the monomers; the heavy group clusters Sn and Pb dimmers are good at this criterion.

Hardness (η) determines the overall stability of the clusters. The harness increases the stability of the system increases. The hardness of the carboranes (**1, 1a**) has higher value around 3.23 to 3.16 than the remaining group-14 clusters. But, in the case of electrophilicity (ω), the carboranes (**1, 1a**) have lower value than the remaining group-14 clusters. The hardness values are gradually decreases from the silaboranes to plumbaboranes.

Softness (S) of the clusters is lower in all geometries except the dimeric plumbaborane (**5**) geometry as 1.30 eV. The higher softness value indicates that the cluster has the possibility to better reactivity. Similarly, the better reactivity of this cluster is supported by the lower energy gap than the remaining group-14 geometries with less hardness and electrophilicity. Hence, we can find the stability and reactivity of the clusters through hardness (η) and softness (S).

Electrophilicity (ω)of the monomeric clusters (**2a, 2, 3a, 4a** and **5a**) are higher than the dimmers except carboranes. In the dimeric system, the silaborane only has the considerable electrophilicity value at 1.01 eV. The dipole moment of the dimeric clusters (**1, 2, 3, 4** and 5) are almost zero and the monomers are in the order of 14.1067 (**5a**) > 9.1407 (**4**a) > 5.4925 (**3a**) > 2.6467 (**1a**) > 0.4212 (**2a**). Among the monomers studied the plumba-*closo*-dodecaborate (**5a**) has highest dipole moment value of 14.1 Debye when compared to the than the remaining group-14 monomeric clusters.

Table 1 DFT calculated chemical descriptors (eV) of the monomers (**1a-5a**) and dimeric clusters (**1-5**) at BP86/Def2-TZVP level.

Cluster	1a	1	2a	2	3a	3	4a	4	5a	5
HOMO	-3.3197	-0.9054	2.3009	-1.4080	1.9679	-1.2635	1.7134	-0.9958	1.9674	-0.7430
LUMO	3.1329	5.4163	6.7607	3.6702	6.8277	3.0466	5.9550	1.8011	5.8040	0.7931
$E_{LUMO-HOMO}$	6.4526	6.3217	4.4598	5.0782	4.8598	4.3101	4.2416	2.7969	3.8368	1.5361
Chemical potential(μ)	-0.0934	2.2555	4.5308	2.2622	4.3978	1.8116	3.8342	0.4026	3.8858	0.0251
Hardness(η)	3.2263	3.1609	2.2299	2.5391	2.4299	2.1551	2.1208	1.3985	1.9184	0.7681
Softness (S)	0.3100	0.3164	0.4485	0.3938	0.4115	0.4640	0.4715	0.7151	0.5213	1.3019
Electrophilicity(ω)	0.0014	0.8047	4.6029	1.0077	3.9797	0.7614	3.4659	0.0580	3.9354	0.0004
Dipole Moment (Debye)	2.65	0.00	0.42	0.03	5.49	0.07	9.14	0.11	14.11	0.17
Ionisation potential(eV)	3.3197	0.9054	-2.3009	1.4080	-1.9679	1.2635	-1.7134	0.9958	-1.9674	0.7430
Electron Affinity (eV)	3.1329	5.4163	-6.7607	-3.6702	-6.8277	-3.0466	-5.9550	-1.8011	-5.8042	-0.7931

3. 3 Polyhedral skeletal electron pair theory (PSEPT) and Cluster valance electron (CVE) count

The skeletal electron pair count and electronic structure of the clusters are studied by PSEPT theory.[49-51] The PSEPT and CVE suggests that the icosahedral borate $[B_{12}H_{12}]^{2-}$ cluster has 13 skeletal electron pair (SEP) possess the *closo* geometry, with the general formula of the *closo* geometry $[B_nH_n]^{2-}$. [45]

12 x 2 (BH) + 2 (2e⁻) = 26 e⁻s

26/2 = 13

SEP = (n+1) = (12+1) = 13

n = 12 (12-vertex icosahedral geometry)

Similarly, the group 14 clusters also posses the *closo* geometry with 13 SEP and n = 12. So, the monomers of the group 14 clusters obeys the wades rule, the geometrical formula of the group 14 clusters are $[B_{11}H_{11}CH]^{1-}$, $[B_{11}H_{11}Si]^{2-}$, $[B_{11}H_{11}Ge]^{2-}$, $[B_{11}H_{11}Sn]^{2-}$ and $[B_{11}H_{11}Pb]^{2-}$.

11 x 2 (BH) + 1 x 3 (C) + 1 (1e⁻) = 26 electrons

11 x 2 (BH) + 1 x 2 (E) + 2 (2e⁻) = 26 electrons   (E = Si, Ge, Sn, Pb)

26/2 = 13

SEP = (n+1) = (12+1) = 13

n = 12

The clusters posses *closo* geometry, but the icosahedral structure is slightly distorted at the hetero atom contained vertex. So, the geometrical structure of the group-14 cluster is distorted icosahedral structure and termed as hetero-*closo*-dodecaborate.

3. 4 Bond Order

The Mayer bond analysis used to determine the bond order and charge density of the atoms. The bond orders of dimeric compounds are given in **Table 2**. The bond order of the E-E bond presents in the carborane is 1.1633, 0.8227 in silaborane, 0.8299 in germaborane, -3.3836 for stannaborane and 0.8944 for plumbaborane clusters. Hence, the bond order of all cluster proves that the bonding interactions presents in the group-14 clusters except stannaboranes. The stannaboranes shows that the negative bond order value in DFT (-3.3836) and DFT-D3 (-0.3721) method. The bond order values obtained from the DFT-D3 methods are slight lower than the DFT method for C and Si systems. But, In the remaining cases, the E-E (Ge, Sn, Pb) bond order is slightly higher than the DFT method. The difference for the Ge cluster is 0.0813 and Sn cluster is 3.0115. For the Pb cluster is DFT-D3 (1.0439) value is higher than the DFT (0.8944) method. The difference between these two methods proves the D3 method is highly favorable for the heavy atoms.

Table 2 The bond order of hetero-*closo*-dodecaborate dimers at BP86/Def2-TZVP level using normal DFT and DFT-D3 method.

Clusters	C		Si		Ge		Sn		Pb	
	DFT	D3	DFT	D3	DFT	D3	DFT	D3	DFT	D3
Mayer	1.1633	1.0373	0.8227	0.7733	0.8299	0.9112	-3.3836	-0.3721	0.8944	1.0439

3. 5 Electronic Structure

The frontier molecular orbitals (FMO) of the clusters studied are provided in the **Figure SF1- Figure SF5**. The highly occupied molecular orbitals (HOMO) of the monomers located at the boron vertices and most of the occupancy flows from upper belt and lower belt to the apical boron vertex. The lowest unoccupied molecular orbitals (LUMO) are highly at the group 14 elements and the boron vertex occupancy also imaged towards the group14 elements. In the dimeric clusters also similar to the monomers, but it has some special electronic structure. The LUMO of the carborane is located in the C-C bonding and centre of the boron cluster. The LUMO+1 and LUMO+2 have the C-C bridging occupancy. the LUMO+4 and LUMO+5 levels shows that the electron flow between two clusters, just like the electron flow from the upper belt of the one carborane cage to another one cage's upper belt boron vertices. The silaborane has Si-Si electron flow at the LUMO and LUMO+1, these cluster slightly tries to flow an electron between two cages. But, the flow is not completed like two cones tries to touching each other. The LUMO+5 is only located inside the two silaborane cages. The germaboranes has the Ge-Ge electron flow at the LUMO+1 and LUMO+2, but the

LUMO+3 has the electron occupancy inside the two cages like LUMO+5 of silaborane. The stannaborane and plumbaborane have the inter-cage electron flow at the HOMO-3 and HOMO-2 levels. The LUMO+1 and LUMO+2 has the electron flow between the E-E bond and the LUMO+3 and LUMO+4 has electron occupancy mostly inside the cages. According to this study, the flow of electrons in the group-14 series is totally different from the top to bottom. In this series, we can categories the electronic structure as three types: 1. Carborane, 2. Silaborane, Germaborane and 3. Stannaborane, plumbaborane.

3. 6 Thermochemistry

The numerical calculations of the monomers and dimers give no imaginary frequency and the obtained optimized geometries also minima in the potential energy surface. The DFT computed free energy of the dimer forming reactions confirming the stable nature of the modelled dimers. So, the clusters have good stability and viable synthesis. The thermal energy desires the product formation is either feasible or not. We can study the thermodynamic features like thermal energy, enthalpy, entropy, Gibbs free energy given in **Table 3** and energy of the reaction for the group14 clusters. The lowest values obtained from the U, H, G factors gives lead to the stability of the geometry. Meanwhile, the entropy (S) also supports the system's thermodynamic stability. The energy of the reactions for the dimmer given in **Table 4**. The borates of silicon, germanium, lead has the energies are -44.5531 kcal/mol, -22.2138 kcal/mol, -25.1631 kcal/mol which indicates that the reactions are feasible at 298.17 K and 1 atm. But, In the case of carborane and stannaborane the energy of the reaction is odd from the remaining clusters, the energy for the reaction is 801.0152 kcal/mol and 2.3835 kcal/mol at the room temperature and 1 atm pressure.

Table 3 DFT calculated thermochemical properties of hetero-*closo*-dodecaborate monomers and dimers at BP86/Def2-TZVP level.

Clusters	Total thermal energy (U)	Enthalpy (H)	Entropy (S)	Gibbs free energy (G)
$[CB_{11}H_{11}]^{1-}$	-318.8699 Eh	-318.8689 Eh	0.03972 Eh	-318.9087 Eh
$[SiB_{11}H_{11}]^{2-}$	-569.6334 Eh	-569.6324 Eh	0.0414 Eh	-569.6738 Eh
$[GeB_{11}H_{11}]^{2-}$	-2357.3931 Eh	-2357.3922 Eh	0.0428 Eh	-2357.4350 Eh
$[SnB_{11}H_{11}]^{2-}$	-494.5461 Eh	-494.5452 Eh	0.0440 Eh	-494.5891 Eh
$[PbB_{11}H_{11}]^{2-}$	-473.1383 Eh	-473.1374 Eh	0.0451 Eh	-473.1824 Eh
$[(CB_{11}H_{11})_2]^{2-}$	-636.4633 Eh	-636.4623 Eh	0.0562 Eh	-636.5185 Eh
$[(SiB_{11}H_{11})_2]^{2-}$	-1139.3379 Eh	-1139.3369 Eh	0.0621 Eh	-1139.3989 Eh
$[(GeB_{11}H_{11})_2]^{2-}$	-4714.8216 Eh	-4714.8207 Eh	0.0649 Eh	-4714.8855 Eh
$[(SnB_{11}H_{11})_2]^{2-}$	-989.0885 Eh	-989.0875 Eh	0.0676 Eh	-989.1551 Eh
$[(PbB_{11}H_{11})_2]^{2-}$	-946.2364 Eh	-946.2354 Eh	0.0708 Eh	-946.3063 Eh

Table 4 DFT calculated Energy of the reaction for hetero-*closo*-dodecaborate dimmers at BP86/Def2-TZVP level.

Clusters	Energy of the reaction
$[(CB_{11}H_{11})_2]^{2-}$	801.0 kcal/mol
$[(SiB_{11}H_{11})_2]^{2-}$	-44.6 kcal/mol
$[(GeB_{11}H_{11})_2]^{2-}$	-22.2 kcal/mol
$[(SnB_{11}H_{11})_2]^{2-}$	2.4 kcal/mol
$[(PbB_{11}H_{11})_2]^{2-}$	-25.2 kcal/mol

3. 7 Spectroscopic Properties

The hetero-*closo*-dodecaborate has three types of protons and borons which lead to three types of chemical shifts (δ) by upper belt (5 B and H), lower belt (5 B and H) and apical vertex. The DFT computed chemical shift values are given in **Table S6-S10**. Usually upper belt borons and protons has lower chemical shift than lower belt and apical position

through the higher shielding effects presents in the upper belt than the remaining. Due to the present of the group-14 heteroatoms, the upper belt vertex obtain higher shielding effect. The difference between the lower belt and upper belt is around 2 to 4 ppm. When comparing these two belts with apical vertex, the chemical shift of apical position is very high. The apical vertex B and H atoms are highly deshielded, these elements utilize higher resonating energy around 4 to10 ppm than the remaining. The calculated values support experimental values of the known clusters and related clusters. [12] [23]

4 Conclusions

The bonding interactions of heteroborates are analyzed by using density functional theory (DFT). The dimeric heteroborate clusters with group-14 element interactions are studied by dispersion correction method (DFT-D3). Although, normal DFT optimization leads to the closer values towards experimentally obtained bond parameters, inclusion of dispersion correlation suggested by Grimmes et.al, improves the metrical parameters significantly (~0.04Å in bond length) towards an experimental value. Further, inclusion of dispersion correction provides the energies more accurately. Dispersion correction using DFT-D3 method provided by Becke-Johnson, improves the energy factor by -93.9685 kcal/mol. Both DFT and experimental studies confirm the more stable nature of the stannaborane dimer **4** with Sn-B bonding interaction. The thermochemistry of the clusters studied, it shows the thermal stability of the newly modelled dimeric clusters (**1-5**) which could have diverse applications. The spectroscopic values are in good agreement with the experimental values.

Supplementary Information

DFT computed metrical paraameters are provided in Tables S1-S5; DFT computed frontier Molecular Orbitals are provided in Figures SF1-SF5; DFT computed NMR chemical shift values are provided in S6-S10.

Data availability

Declarations

References
1. Power PP (1999) π-Bonding and the Lone Pair Effect in Multiple Bonds between Heavier Main GroupElements. Chem Rev 99:3463–3504. https://doi.org/10.1021/cr9408989
2. Klinkhammer KW, Schwarz W (1995) Bis(hypersilyl)tin and Bis(hypersilyl)lead, Two Electron-Rich Carbene Homologs. Angew Chem Int Ed Engl 34:1334–1336. https://doi.org/10.1002/anie.199513341
3. Zhiyuan He, Lingyu Liu, Felix J. de Zwart, Xiaolian Xue, Andreas W. Ehlers, KaKing Yan, Serhiy Demeshko, Jarl Ivar van der Vlugt, Bas de Bruin, and Jeremy Krogman (2022) Reactivity of a Unique Si(I)–Si(I)-Based η^2-Bis(silylene) Iron Complex. Inorg Chem 61(30):11725-11733. https://doi.org/10.1021/acs.inorgchem.2c01369
4. Stürmann M, Saak W, Klinkhammer KW, Weidenbruch M (1999) A Heteroleptic (E)-1,2-Diaryl-1,2-disilyldistannene without Donor Stabilization. Z anorg allg Chem 625:1955–1956. https://doi.org/10.1002/(SICI)1521-3749(199912)625:12<1955::AID-ZAAC1955>3.0.CO;2-J
5. Bashkurov R, Fridman N, Bravo-Zhivotovskii D, Apeloig Y (2023) The First Planar, Not Twisted, Distannene − A Structural Alkene Analog. Synthesis, Isolation and X-ray Crystallography Characterization. Chemistry A European J 29:e202302678. https://doi.org/10.1002/chem.202302678
6. Davidson PJ, Harris DH, Lappert MF (1976) Subvalent Group 4B Metal Alkyls and Amides. Part I. The Synthesis and Physical Properties of Kinetically Stable Bis[bis(trimethysilyl)methyl]- germanium(ii), -tin(ii), and -lead(ii) t
7. Klinkhammer KW, Fässler TF, Grützmacher H (1998) The Formation of Heteroleptic Carbene Homologues by Ligand Exchange-Synthesis of the First Plumbanediyl Dimer. Angewandte Chemie International Edition 37:124–126. https://doi.org/10.1002/(SICI)1521-3773(19980202)37:1/2<124::AID-ANIE124>3.0.CO;2-C
8. Wang S, Li H-J, Kuo T-S, Shen L-C, Liu H-J (2021) Ambiphilic Nature of Dipyrrolylpyridine-Supported

Divalent Germanium and Tin Compounds. Organometallics 40:3659–3667. https://doi.org/10.1021/acs.organomet.1c00494

9. Nagase S (2012) Multiple bonds between lead atoms and short bonds between transition metals. Pure and Applied Chemistry 85:649–659. https://doi.org/10.1351/PAC-CON-12-08-04

10. Guo J-D, Liptrot DJ, Nagase S, Power PP (2015) The multiple bonding in heavier group 14 element alkene analogues is stabilized mainly by dispersion force effects. Chem Sci 6:6235–6244. https://doi.org/10.1039/C5SC02707A

11. Körbe S, Schreiber PJ, Michl J (2006) Chemistry of the Carba- *closo* -dodecaborate(−) Anion, CB $_{11}$ H $_{12}$ $^{-}$. Chem Rev 106:5208–5249. https://doi.org/10.1021/cr050548u

12. Gädt T, Wesemann L (2007) Stanna- *closo* -dodecaborate Chemistry. Organometallics 26:2474–2481. https://doi.org/10.1021/om061042k

13. Roy RK, Krishnamurti S, Geerlings P, Pal S (1998) Local Softness and Hardness Based Reactivity Descriptors for Predicting Intra- and Intermolecular Reactivity Sequences: Carbonyl Compounds. J Phys Chem A 102:3746–3755. https://doi.org/10.1021/jp973450v

14. Aizman A, Contreras R, Pérez P (2005) Relationship between local electrophilicity and rate coefficients for the hydrolysis of carbenium ions. Tetrahedron 61:889–895. https://doi.org/10.1016/j.tet.2004.11.014

15. Morell C, Grand A, Toro-Labbé A (2006) Theoretical support for using the Δf(r) descriptor. Chemical Physics Letters 425:342–346. https://doi.org/10.1016/j.cplett.2006.05.003

16. Cárdenas C, Rabi N, Ayers PW, Morell C, Jaramillo P, Fuentealba P (2009) Chemical Reactivity Descriptors for Ambiphilic Reagents: Dual Descriptor, Local Hypersoftness, and Electrostatic Potential. J Phys Chem A 113:8660–8667. https://doi.org/10.1021/jp902792n

17. Padmanabhan J, Parthasarathi R, Elango M, Subramanian V, Krishnamoorthy BS, Gutierrez-Oliva S, Toro-Labbe A, Roy DR, Chattaraj PK (2007) Multiphilic Descriptor for Chemical Reactivity and Selectivity. J Phys Chem A 111:9130–9138. https://doi.org/10.1021/jp0718909

18. Morell C, Grand A, Toro-Labbé A (2005) New Dual Descriptor for Chemical Reactivity. J Phys Chem A 109:205–212. https://doi.org/10.1021/jp046577a

19. Cárdenas-Jirón GI, Gutiérrez-Oliva S, Melin J, Toro-Labbé A (1997) Relations between Potential Energy, Electronic Chemical Potential, and Hardness Profiles. J Phys Chem A 101:4621–4627. https://doi.org/10.1021/jp9638705

20. Mulliken R S (1952) Molecular Compounds and their Spectra II, Journal of American Chemical Society 74(3):811-824. https://doi.org/10.1021/ja01123a067

21. Kar T, Scheiner S, Sannigrahi AB (1998) Ab initio calculations of hardness and chemical potential of open shell systems using SCF, MP2 and MP4 methods. Journal of Molecular Structure: THEOCHEM 427:79–85. https://doi.org/10.1016/S0166-1280(97)00172-3

22. Luo J, Xue ZQ, Liu WM, Wu JL, Yang ZQ (2006) Koopmans' Theorem for Large Molecular Systems within Density Functional Theory. J Phys Chem A 110:12005–12009. https://doi.org/10.1021/jp063669m

23. Gädt T, Dimmer J-A, Fleischhauer S, Frank A, Nickl C, Wutz T, Eichele K, Wesemann L (2015) Oxidation of germa- and stanna-closo-dodecaborate. Dalton Trans 44:4726–4731. https://doi.org/10.1039/C5DT00099H

24. Brindha V, Krishnamoorthy BS (2024) Isomer Preferences and Structural Studies on Cobaltaboranes – A Theoretical Investigation. Biointerface Reseach in Applied Chemistry 14(3):73. https://doi.org/10.33263/BRIAC143.073

25. Nagalakshmi V, Nandhini R, Brindha V, Krishnamoorthy BS, Balasubramani K (2020) Half-sandwich ruthenium(II) complexes containing biphenylamine based Schiff base ligands: Synthesis, structure and catalytic activity in amidation of various aldehydes. Journal of Organometallic Chemistry 912:121175. https://doi.org/10.1016/j.jorganchem.2020.121175

26. Gomathi S, Kavitha K, Savitha N, Mohana A, Brindha V, Krishnamoorthy BS (2022) Molecular Structure, Reactivity and Spectroscopic Properties of Hallucinogens Psilocybin, Mescaline and their Derivatives – A Computational Study. Lett Appl Nano Bio Sci 12:105. https://doi.org/10.33263/LIANBS124.105

27. Neese F (2022) Software update: The ORCA program system—Version 5.0. WIREs Comput Mol Sci 12:e1606. https://doi.org/10.1002/wcms.1606

28. Vosko SH, Wilk L, Nusair M (1980) Accurate spin-dependent electron liquid correlation energies for local spin density calculations: a critical analysis. Can J Phys 58:1200–1211. https://doi.org/10.1139/p80-159

29. Becke AD (1986) Density functional calculations of molecular bond energies. The Journal of Chemical Physics

84:4524–4529. https://doi.org/10.1063/1.450025

30. Becke AD (1988) Density-functional exchange-energy approximation with correct asymptotic behavior. Phys Rev A 38:3098–3100. https://doi.org/10.1103/PhysRevA.38.3098

31. Perdew JP (1986) Density-functional approximation for the correlation energy of the inhomogeneous electron gas. Phys Rev B 33:8822–8824. https://doi.org/10.1103/PhysRevB.33.8822

32. Krishnamoorthy BS, Thakur A, Chakrahari KKV, Bose SK, Hamon P, Roisnel T, Kahlal S, Ghosh S, Halet J-F (2012) Theoretical and Experimental Investigations on Hypoelectronic Heterodimetallaboranes of Group 6 Transition Metals. Inorg Chem 51:10375–10383. https://doi.org/10.1021/ic301571e

33. Krishnamoorthy BS, Kahlal S, Ghosh S, Halet J-F (2013) Electronic, geometrical, and thermochemical studies on group-14 element-diruthenaborane cluster compounds: a theoretical investigation. Theor Chem Acc 132:1356. https://doi.org/10.1007/s00214-013-1356-6

34. Krishnamoorthy BS, Kahlal S, Le Guennic B, Saillard J-Y, Ghosh S, Halet J-F (2012) Molecular transition-metal boron compounds. Any interest? Solid State Sciences 14:1617–1623. https://doi.org/10.1016/j.solidstatesciences.2012.03.026

35. Weigend F, Ahlrichs R (2005) Balanced basis sets of split valence, triple zeta valence and quadruple zeta valence quality for H to Rn: Design and assessment of accuracy. Phys Chem Chem Phys 7:3297. https://doi.org/10.1039/b508541a

36. Grimme S, Antony J, Ehrlich S, Krieg H (2010) A consistent and accurate *ab initio* parametrization of density functional dispersion correction (DFT-D) for the 94 elements H-Pu. The Journal of Chemical Physics 132:154104. https://doi.org/10.1063/1.3382344

37. Grimme S, Ehrlich S, Goerigk L (2011) Effect of the damping function in dispersion corrected density functional theory. J Comput Chem 32:1456–1465. https://doi.org/10.1002/jcc.21759

38. Johnson ER, Becke AD (2006) A post-Hartree-Fock model of intermolecular interactions: Inclusion of higher-order corrections. The Journal of Chemical Physics 124:174104. https://doi.org/10.1063/1.2190220

39. Johnson ER, Becke AD (2005) A post-Hartree-Fock model of intermolecular interactions. The Journal of Chemical Physics 123:024101. https://doi.org/10.1063/1.1949201

40. Mareš J, Vaara J (2018) *Ab initio* paramagnetic NMR shifts *via* point-dipole approximation in a large magnetic-anisotropy Co(II) complex. Phys Chem Chem Phys 20:22547–22555. https://doi.org/10.1039/C8CP04123G

41. Safi ZS, Wazzan N (2022) DFT calculations of ^{1}H- and ^{13}C-NMR chemical shifts of 3-methyl-1-phenyl-4-(phenyldiazenyl)-1H-pyrazol-5-amine in solution. Scientific Reports 12:17798. https://doi.org/10.1038/s41598-022-22900-y

42. Becker ED (2000) High Resolution NMR : Theory and Chemical Applications, 3rd Edition ISBN: 9780120846627. https://doi.org/10.1016/B978-0-12-084662-7.X5044-3

43. Chattaraj PK, Maiti B, Sarkar U (2003) Philicity: A Unified Treatment of Chemical Reactivity and Selectivity. J Phys Chem A 107:4973–4975. https://doi.org/10.1021/jp034707u

44. Roy DR, Parthasarathi R, Padmanabhan J, Sarkar U, Subramanian V, Chattaraj PK (2006) Careful Scrutiny of the Philicity Concept. J Phys Chem A 110:1084–1093. https://doi.org/10.1021/jp053641v

45. Allen FH, Kennard O, Watson DG, Brammer L, Orpen AG, Taylor R (1987) Tables of bond lengths determined by X-ray and neutron diffraction. Part 1. Bond lengths in organic compounds. J Chem Soc, Perkin Trans 2 S1. https://doi.org/10.1039/p298700000s1

46. Fink MJ, Michalczyk MJ, Haller KJ, et al X-ray Crystal Structure for Two Disilenes

47. Sasamori T, Han JS, Hironaka K, et al (2010) Synthesis and structure of stable 1,2-diaryldisilyne. Pure and Applied Chemistry 82:603–612. https://doi.org/10.1351/PAC-CON-09-08-02

48. Lee VYa, Fukawa T, Nakamoto M, et al (2006) (^{t}Bu$_2$MeSi)$_2$SnSn(SiMe^{t}Bu$_2$)$_2$: A Distannene with a >SnSn< Double Bond That is Stable Both in the Solid State and in Solution. J Am Chem Soc 128:11643–11651. https://doi.org/10.1021/ja063322x

49. Wade K (1976) Structural and Bonding Patterns in Cluster Chemistry. In: Advances in Inorganic Chemistry andRadiochemistry. Elsevier, pp 1–66

50. Wade K (1971) The structural significance of the number of skeletal bonding electron-pairs in carboranes, the higher boranes and borane anions, and various transition-metal carbonyl cluster compounds. J Chem Soc D 792. https://doi.org/10.1039/c29710000792

51. Mingos DMP (1972) A General Theory for Cluster and Ring Compounds of the Main Group and Transition Elements. Nature Physical Science 236:99–102. https://doi.org/10.1038/physci236099a0

Supplementary Files

This is a list of supplementary files associated with this preprint. Click to download.

- supportinginformation.docx